Journal of Controlled Release 252 (2017) 18–27

Contents lists available at ScienceDirect

Journal of Controlled Release

journal homepage: www.elsevier.com/locate/jconrel

New drug candidates for liposomal delivery identified by computer modeling of liposomes' remote loading and leakage

Ahuva Cern [a,b,*], David Marcus [c], Alexander Tropsha [d], Yechezkel Barenholz [a,1], Amiram Goldblum [b,1]

[a] Laboratory of Membrane and Liposome Research, Department of Biochemistry, IMRIC, The Hebrew University - Hadassah Medical School, Jerusalem, Israel
[b] Molecular Modeling and Drug Design Laboratory, The Institute for Drug Research, The Hebrew University of Jerusalem, Israel
[c] European Molecular Biology Laboratory, European Bioinformatics Institute (EMBL–EBI), Wellcome Trust Genome Campus, Hinxton, Cambridge CB10 1SD, United Kingdom
[d] The Laboratory for Molecular Modeling, UNC Eshelman School of Pharmacy, University of North Carolina at Chapel Hill, NC, USA

ARTICLE INFO

Article history:
Received 10 January 2017
Accepted 14 February 2017
Available online 16 February 2017

Keywords:
Iterative Stochastic Elimination
Structural descriptors
Liposomes- based nano-drugs
Liposome stability to leakage

ABSTRACT

Remote drug loading into nano-liposomes is in most cases the best method for achieving high concentrations of active pharmaceutical ingredients (API) per nano-liposome that enable therapeutically viable API-loaded nano-liposomes, referred to as nano-drugs. This approach also enables controlled drug release. Recently, we constructed computational models to identify APIs that can achieve the desired high concentrations in nano-liposomes by remote loading. While those previous models included a broad spectrum of experimental conditions and dealt only with loading, here we reduced the scope to the molecular characteristics alone. We model and predict API suitability for nano-liposomal delivery by fixing the main experimental conditions: liposome lipid composition and size to be similar to those of Doxil® liposomes. On that basis, we add a prediction of drug leakage from the nano-liposomes during storage. The latter is critical for having pharmaceutically viable nano-drugs. The "load and leak" models were used to screen two large molecular databases in search of candidate APIs for delivery by nano-liposomes. The distribution of positive instances in both loading and leakage models was similar in the two databases screened. The screening process identified 667 molecules that were positives by both loading and leakage models (i.e., both high-loading and stable). Among them, 318 molecules received a high score in both properties and of these, 67 are FDA-approved drugs. This group of molecules, having diverse pharmacological activities, may be the basis for future liposomal drug development.

1. Introduction

Liposomes are a leading drug delivery system for parenteral use. Since the first liposomal drug, Doxil® which was approved by the FDA in 1995 [1,2], 13 more liposomal drugs were approved by the FDA, half of which are nano-drugs [3]. More liposomal drugs are now in clinical trials [4,5]. Nano-liposomes are efficacious for treating a number of cancers; infectious diseases (bacterial [6], fungal [7], and viral [8,9]); and neurodegenerative and inflammatory disorders [10]. In these diseases nano-liposomes utilize the enhanced permeability and retention (EPR) effect and deliver the drug selectively to the diseased tissues [11–14]. Most active pharmaceutical ingredients (APIs) are not suitable for "passive" loading into nano-liposomes as this loading method does not achieve the desired API concentration in the nano-liposomes required for sufficient therapeutic efficacy in humans [15]. In order to obtain a viable nano-drug formulation, the API should fulfill several conditions: (i) the concentration of the drug in the nano-liposomes should be high enough for administering a therapeutic dose for human treatment, (ii) the liposomal nano-drug product should be stable upon storage, and (iii) drug release in blood circulation in vivo should be slow to enable distribution of enough drug-loaded liposomes to the target (disease) site, where the drug should be released at therapeutically significant levels [15].

Nano-liposomes have an extremely small (nano) internal volume. A single PEGylated nano-liposome before remote loading of doxorubicin has a trapped aqueous volume, measured by cryo-transmission electron microscopy, of $133 \pm 18\ nm^3 \cdot 10^3$, which after remote loading of doxorubicin increases to $150 \pm 20\ nm^3 \cdot 10^3$ (our unpublished data). This makes passive loading of most drugs a non-viable option, as a therapeutically sufficient quantity of drug loading required for human treatment cannot be reached. The method of remote (active) loading was developed to overcome this major obstacle and to reach a sufficiently high intra-liposomal drug concentration of several hundred mM [16–18]. Remote loading is based on the use of liposomes exhibiting ion and/or proton gradients as the driving force for getting drugs into liposomes. This loading method requires the drug to be an amphipathic weak base [16,18,19] or weak acid [20]. An ammonium ion gradient is used

* Corresponding author.
E-mail addresses: ahuva.cern@mail.huji.ac.il (A. Cern), chezyb@ekmd.huji.ac.il (Y. Barenholz), amiramg@ekmd.huji.ac.il (A. Goldblum).
[1] Equal senior authors.

http://dx.doi.org/10.1016/j.jconrel.2017.02.015
0168-3659/

successfully for the remote loading of amphipathic weak bases [16,18,21], while an acetate gradient is very effective for the remote loading of amphipathic weak acids [22–25]. Remote loading is important, not only for drug loading into liposomes, but also for retaining the drug inside the liposomes. Recently it has become clear that remote loading is also important to achieve controlled drug release at the disease site [1,2,26]. In some cases, APIs that are not amphipathic weak acids or bases can be chemically modified to amphipathic weak acid or base prodrugs in order to be remote loaded to liposomes. Such is the case with steroids modified to their hemisuccinate derivatives, which are amphipathic weak acids and are converted upon their release to the active steroid [22,27,28]. Another approach to load non-amphipathic weak acids or bases by remote loading is to complex the drug with cyclodextrins which are amphiphatic weak acides or bases by themselves that can be remotely loaded as a drug-cyclodextrin complex to liposomes [29].

Not all molecules that are amphipathic weak acids or bases fulfill the conditions required for having high enough drug concentration in liposomes sufficient for human treatment. The availability of a large data collection gathered on liposomal remote loading in-house (at the Barenholz lab, described in [18]) and from the literature, enabled us recently to develop Quantitative Structure–Property Relationship (QSPR) models that were used to predict drug suitability for remote loading in terms of loaded intra-liposome drug concentrations [23,30]. This previous model used hybrid descriptors composed of experimentally derived descriptors (EDD) such as lipid composition and liposomes' size (9 descriptors) and descriptors related to the molecular properties of the drugs (184 descriptors) calculated from the 2-dimensional molecular structures by suitable software. We demonstrated that computational models are capable of identifying molecules that could achieve the desired loaded drug concentration [23]. The models were validated experimentally, as we showed that drugs prioritized and selected from a large drug library or from previous literature sources, indeed had the predicted loading capacity [23]. The issue of stability upon storage (shelf life) of the loaded nano-liposomes was not dealt with in our previous papers. It is however critical to the viability of such liposomal nano-drugs.

Following these first attempts to model drug suitability for remote liposomal loading and their use for screening molecules, a few drawbacks of the model were found: the dependence of the model on EDD, the relatively narrow classification of good candidates, and the lack of prediction of the essential component of leakage (to predict shelf life stability).

In the present study, we aim to improve the previous model by addressing these drawbacks. We created models that focus on the characteristics of the API, while keeping formulation properties constant. This was done by limiting the dataset used for modeling only for a narrow range of lipid composition of nano-liposomes. The formulation features selected are high-T_m liposome forming phosphatidylcholine (PC ≥ 37 °C) and high mole% cholesterol, which is the most common lipid composition for liposomal formulations currently used and most of the available data are related to this range of lipid composition [3]. In addition, the previous narrow classification of a "good candidate" was modified to include more molecules. Leakage upon storage might be a major source of instability of liposomal formulations. Therefore, we have similarly modeled stability related to leakage of API from nano-liposomes during storage which is based on molecular descriptors alone. From a computational perspective, it is advantageous to restrict experimental conditions because of the limited number of experimental conditions known for each molecule. From the liposome technology experience, it may be assumed that an API that is efficiently loaded to liposomes based on high-T_m liposomes' "forming lipids" will also show high loading to low-T_m liposomes [21] although this assumption requires a case per case evaluation.

Leakage of drugs from liposomes is important to model for many reasons. It might critically limit the shelf-life stability of the liposomal product and it is relevant to in vivo integrity, which is the basis for its superior pharmacokinetic (PK) and biodistribution profile of the drug delivered via the nano-liposomes. The superior PK profile is to a large extent responsible for the superior performance of such nano-liposomes based nano-drug [3,31]. The parameters that affect drug leakage upon storage are derived from the physicochemical properties of the drug and the liposomal composition as well as the storage medium and storage temperature. The in vivo leakage (also termed in vivo release) which is required for therapeutic efficacy is a complex process. This process is influenced by the liposomal composition and the biological environment reached by the liposomes, which for blood includes among others factors such as blood-hemodynamics, interaction with blood cells and with plasma lipoproteins, interactions with different opsonines and large dilution-induced release. In this study, we focused on the leakage related only to shelf-life stability and, as described earlier, on the loading; the models were constructed based on molecular descriptors (properties) only.

Models that predict both loading and stability of liposomal drugs present the most important properties for the suitability of a drug for nano-liposomal delivery. The models generated in this study were used for screening two large molecular libraries: the Comprehensive Medicinal Chemistry (CMC) and Drug Bank (DB) databases, containing together 13,700 unique molecules having biological activity. A group of 667 molecules was found to have the loading and leakage properties required by candidates for liposomal delivery. Of this group, 318 molecules received the highest score in both properties. Of those high-scored molecules, 67 are FDA-approved drugs. This group of molecules, having diverse pharmacological activities, may be the basis for future liposomal drug development.

2. Methods

2.1. Dataset preparation

The present study was aimed at modeling two characteristics of liposomal drugs: drug loading and drug leakage upon storage. Two datasets were therefore collected and used to model each characteristic. The data were collected from the literature and from in-house data of the Barenholz lab. The data collected are presented in Supplementary Tables S1 and S2.

2.1.1. Descriptors

For each molecule in the datasets, molecular descriptors were calculated using the Molecular Operating Environment (MOE) software [32]; A complete list of descriptors is given in Supplementary Table S3.

2.1.2. Loading dataset

Molecules were included in the dataset only if their remote loading was tested for liposomes containing high-mole% cholesterol (≥30%) and high-Tm phospholipid (≥37 °C). Based on previous information, 30% is the lowest mole% cholesterol that avoids extensive leakage of the formulation at 37 °C [33]. Some negative instances were added to the dataset although loaded to low-Tm liposomes. This was done only in cases of loading efficiency of not >50%. Loading efficiency is assumed not to be affected by membrane composition as long as the loading is performed at a temperature above the Tm of the phospholipid [21]. However, due to leakage that may occur rapidly for low-Tm lipids (for which storage temperature is close to the Tm), leakage may occur from the time of loading to the time of analysis. Therefore, we could not always assume that low loading to low-Tm membranes will also be low loading to high-Tm membranes. Negative instances that were low loaded to low-Tm membranes were therefore entered to the dataset only if their loading was not borderline, i.e., in cases of not >50% loading efficiency at a drug/lipid (D/L) mole ratio of ≤0.2.

The classification of positive instances was slightly changed (compared to the previous study [30]) to broaden the criteria for positive instances. In the previous study, positive instances (high loading) were those having ≥70% loading efficiency at D/L mole ratio of ≥0.3. In the

present study we added to the group of positive instances those that showed ≥90% loading efficiency at D/L ratio of ≥0.2. This classification is based on liposomal product requirements. By assuming a 150 mg dose of an API having a molecular weight of 500 Da that is needed to be administered in 100 ml infusion volume (higher volumes will result in longer infusion time and higher lipid administration) results in a required encapsulated drug concentration of 3.0 mM. Assuming hydrogenated soy phosphatidylcholine (HSPC) concentration of 12 mM (as found in Doxil®) results in a D/L ratio of 0.25. In addition, the influence of the threshold selected on model performance was tested as described in Section. 3.1.

The final loading dataset consisted of 67 molecules from the literature [17,24,34–80] and from in-house data (compared to the 46 molecules in the previous study [30]), of which 23 were classified as positives (high loading) and 44 were classified as negatives (low loading). The loading dataset is presented in Supplementary Table S1.

2.1.3. Leakage dataset

Leakage upon storage is a characteristic of a liposomal drug that determines an important aspect of its shelf-life stability. In terms of stability, a drug product should retain >90% of label claim of potency over its shelf-life period when stored at recommended conditions [81]. Liposomes are usually stored at refrigerator conditions, and therefore drug leakage of <10% over 1 year of storage at 4 °C would represent a stable product in terms of drug leakage. However, the data collected consisted of many different assays to evaluate drug leakage other than storage stability. The experimental data collected were first evaluated to contain only assays that were predictive of storage stability.

Based on the above regulation, and the data available, molecules were classified as positives (slow leaking) and negatives (rapid leaking) based on their leakage over time from rigid membrane liposomes containing high mole% cholesterol (≥30%). Slow leaking instances were those showing lower than 10% leakage at 4 °C in more than a month, or at higher temperature (25 °C or 37 °C) in >24 h. Rapid leaking instances were those showing >10% leakage at 4 °C in less than a month, or at higher temperature in <24 h. No other classification for slow or rapid leaking instances could apply. Note that two instances, showing slow leakage, tested in the presence of plasma were added to the dataset [52]. In these cases, the liposomal formulation was PEGylated, assuming that slow leaking in plasma will probably show slow leaking without plasma. In most cases plasma protein binding to liposomes was shown to decrease liposomal stability [82]. However, a few cases reported the opposite, showing that plasma protein increased liposomal stability [83]. The two cases used in our dataset were PEGylated, and there is a low chance that the plasma proteins will stabilize this membrane. We therefore assumed that in these cases slow leaking in the presence of plasma will show slow leaking also upon storage. The final leakage dataset consisted of 27 molecules from the literature [24,36,37,45–47,52,54,57,60,61,65,70,73,75,76,84–87] and from in-house data. Of these, 15 molecules were classified as slow leaking (positives) and 12 were classified as rapid leaking (negatives). Leakage dataset is presented in Supplementary Table S2. Twenty-three molecules in the leakage dataset (out of 27) were also included in the loading dataset. Most of the molecules that were positives (slow leaking) in leakage were also positives (high loading) in loading and vice versa.

2.2. Computational methods

2.2.1. Iterative Stochastic Elimination (ISE) [88]

ISE is a search and optimization method for extremely complex combinatorial problems. Among others, ISE can optimize the selection of filters that are able to distinguish between molecules from different activity classes. Each filter contains 4 or 5 ranges of different molecular properties ("descriptors"), and filters differ from each other by their ability to distinguish between activity classes.

The process of optimization begins with a large set of variables each having many values, starting with a huge number of possible combinations of variables and values that may be larger than 10^{100}. That huge number is reduced in iterations to a manageable number of combinations, in the millions or less, which are exhaustively calculated and sorted based on scoring. Application of ISE thus produces a model that is constructed of a set of best scored filters. Once such a model has been produced, the ranking index of any other molecule may be determined by its ability to pass (or fail to pass) that model's filters. A molecule is scored by combining these filters' weights (adding upon passage, subtracting upon failure to pass) to create a normalized index whose values are between −1 (negative) and +1 (positive). Molecules that pass more filters receive a higher index. The ranking model calculation is composed of the following steps:

- Single range optimization— finding the best ranges of each separate descriptor that maximize the ability to distinguish between two classes. 186 descriptors were calculated by MOE for each molecule, of which highly correlated ones and descriptors with very low standard deviations were eliminated, ending in some 150 final descriptors.
- Filters optimization —a filter is produced by combining ranges of a few descriptors, whose total number is given at the outset, and is usually 4 or 5. Each filter is picked by a random choice of descriptors and scored based on its ability to distinguish between actives (which can be predicted correctly as "True Positives", TP or wrongly as "False Negatives", FN) and decoys (predicted correctly are "True Negatives", TN or wrongly as "False Positives", FP) from the learning set. The Matthews Correlation Coefficient (MCC, Eq. (1) below), uses the results of these four criteria (TP, FN, TN, FP) to score each randomly picked filter, and once a huge sample of filters has been scored, ISE examines each descriptor and eliminates descriptors' ranges that contribute consistently to the worst MCC scores. This constitutes a single iteration. Sampling and eliminations continue in iterations to a point where the total number of combinations (usually $<10^6$) allows to compute exhaustively all remaining combinations.

$$MCC = \frac{TP \times TN - FP \times FN}{\sqrt{(TP+FP) \times (TP+FN) \times (TN+FP) \times (TN+FN)}} \quad \text{Eq. 1}$$

where TP and TN are true positives and true negatives, respectively, and FN and FP are false positives and false negatives, respectively.

- Constructing the model— it is now possible to sort all the combinations based on their MCC values, subsequently to cluster the top filters, which constitute the "Model".
- Virtual screening — The model is used to score any number of molecules following the calculation of their molecular descriptors. Each set of a molecule's descriptors is tested whether it passes or not through each and every filter of the model. It gains score by passing a filter but loses score if not. The final score for a molecule is a result of a balance between those filters passed successfully and those that were not successfully passed. A normalized score takes into account the total number of filters. Each molecule thus gets an ISE index that enables one to sort the results and pick the best (top-scored) molecules (Eq. (2)).

$$Index = \frac{\sum_{i=1}^{n} \delta i_{active} \frac{P_{TPi}}{P_{FPi}} - \delta i_{inactive} \frac{P_{TNi}}{P_{FNi}}}{n} \quad \text{Eq. 2}$$

In Eq. (2), n is the number of filters, δactive = 1 if the molecule passed filter i as a positive, otherwise δactive = 0. δinactive = 1 if a molecule passed a filter as a negative, otherwise δinactive = 0. P_{TP}/P_{FP} is the proportion of true to false positives in a particular filter and may be

called an efficiency factor, whereas P_{TN}/P_{FN} is an inefficiency factor and the proportion of true negatives versus false negatives.

2.2.2. External validation

Loading models were built under a 5-fold external validations scheme: the dataset was randomly divided into five groups of nearly equal size; four groups were combined and used iteratively as training sets, and the fifth group was employed as a test set. Final scores of the learning set are thus based on each molecule being once in a test set.

Leakage dataset is a relatively small dataset (27 molecules); for that reason, the Leave One Out (LOO) validation scheme was employed. In this process, models were built with 26 molecules, and one molecule was tested as external. The process was repeated 27 times so that each molecule was tested once as being "external".

To characterize the predictive power of models, we used the following statistics:

$$\text{Sensitivity} = \text{TP}/(\text{TP} + \text{FN}), \text{and}$$

$$\text{Specificity} = \text{TN}/(\text{TN} + \text{FP}).$$

Correct classification rate (CCR) was defined as follows:

$$\text{CCR} = 0.5 \times (\text{Sensitivity} + \text{Specificity})$$

2.3. Databases screening

Two databases were used for screening:

1. Comprehensive Medicinal Chemistry (CMC) database containing 8402 molecules (after removing duplicate molecules) that are used or have been studied as medicinal agents in humans, pharmacological agents, or biologically active compounds.
2. Drug bank (DB) database containing 6831 drug entries (after removing duplicate molecules) including FDA-approved small molecule drugs, FDA-approved biotech drugs, nutraceuticals, or experimental drugs.

There is a total of 13,700 unique molecules (after subtracting 1533 molecules that are common to both databases).

The databases were screened by both loading and leakage models after calculating structural descriptors for each molecule in the two databases. For the purpose of comparison, the databases were also screened by the previous loading model [30] (consisting of hybrid descriptors (EDD) and structural descriptors). The EDD used were those corresponding to the formulation of Doxil.

3. Results and discussion

Previously, we published a QSPR model to predict the loading of a drug by remote liposomal loading [30]. Using that model for screening and testing the suitability of APIs revealed a few drawbacks of the model: its dependence on EDD, the relatively narrow classification of good candidates, and the lack of modeling the leakage. In this study we therefore aimed to improve our previous model by:

(1) Simplifying the computation and modeling. We developed the models to be independent of formulation properties (EDD) by keeping liposome composition and size distribution similar to Doxil, while focusing only on the properties of the loaded molecules as descriptors. Namely, only nano-liposomes composed of high-Tm phospholipid (>37 °C) and high mole% cholesterol (≥30%) were included. Molecules in the dataset were classified as "high" loaded or "low" loaded based on their loading only to such nano-liposomes. In addition, the number of molecules used for loading model building was increased from 47 to 67 molecules.
(2) The classification of positive instances was broadened to include instances that showed ≥90% loading efficiency at D/L ratio of ≥0.2.
(3) Leakage upon storage was modeled to enable screening of molecules for that important aspect of liposomal activity.

The following sections describe the modeling of loading and leakage properties based on structural descriptors, as well as the results of the virtual screening of the two databases by these models.

3.1. Loading model

The loading dataset was modeled by ISE employing the 5-fold external validation scheme. Several thresholds were used for classification of positive instances:

1. Loading efficiency of ≥70% at D/L ratio of ≥0.1.
2. Loading efficiency of ≥70% at D/L ratio of ≥0.2.
3. Loading efficiency of ≥70% at D/L ratio of ≥0.3.
4. Loading efficiency of ≥70% at D/L ratio of ≥0.3 and ≥90% at D/L ratio of ≥0.2.

The confusion matrices for the external validation of the four classification thresholds are presented in Table 1. The classification based on 0.1 threshold resulted in the best predictability parameters with a specificity of 0.87 and sensitivity of 0.75. Increasing the threshold to 0.2 and 0.3 did not significantly change the specificity but showed lower sensitivity of the models. The 0.2/0.3 threshold (no. 4 above) resulted in the highest specificity (0.89) and low sensitivity (0.52). Our model is aimed to identify molecules suitable for nano-liposomal delivery system and as such molecules having high loading efficiency at D/L ratio of 0.1 will only apply for highly potent drugs. We selected the 0.2/0.3 threshold for identifying suitable molecules for this delivery system because it complies with the usual dosing requirements of a nano-liposomal formulation and it showed high specificity. Using this model for candidate's identification has low chances for false positive instances while the low sensitivity points out that many good candidates will not be identified. The development of a nano-liposomal drug is a major undertaking which requires much time and therefore our main aim in this model building is to have the lowest possible number of false positive instances, while false negative instances are less of a problem. The index distribution of the externally validated molecules of the model built with the 0.2/0.3 classification are shown in Fig. 1. This figure shows a trend in the results. At the extreme indexes, ≥0.5 and ≤−0.5, there is a better classification in terms of low content of false negatives and false positives. Our aim is to identify true positive molecules and avoid false positive instances. According to Fig. 1, 29% (5/17) of the molecules indexed above zero are false positives, and this value decreases

Table 1
Five-fold cross validation of different thresholds in the loading model.

Classification								
	0.1[a]		0.2[b]		0.3[c]		0.2/0.3[d]	
	Obs low	Obs high	Obs low	Obs high	Obs low	Obs high	Obs low	Obs high
Pred low	34	7	34	8	49	7	39	11
Pred high	5	21	8	17	9	2	5	12
% Correctly classified	82.09		76.12		6.12		76.12	
CCR	0.81		0.74		0.53		0.7	
Specificity	0.87		0.81		0.84		0.89	
Sensitivity	0.75		0.68		0.22		0.52	

Pred- Predicted, Obs- Observed.
[a] High instances are defined as having loading efficiency of ≥70% at D/L ratio of ≥0.1.
[b] High instances are defined as having Loading efficiency of ≥70% at D/L ratio of ≥0.2.
[c] High instances are defined as having Loading efficiency of ≥70% at D/L ratio of ≥0.3.
[d] High instances are defined as having Loading efficiency of ≥70% at D/L ratio of ≥0.3 and ≥90% at D/L of ≥0.2.

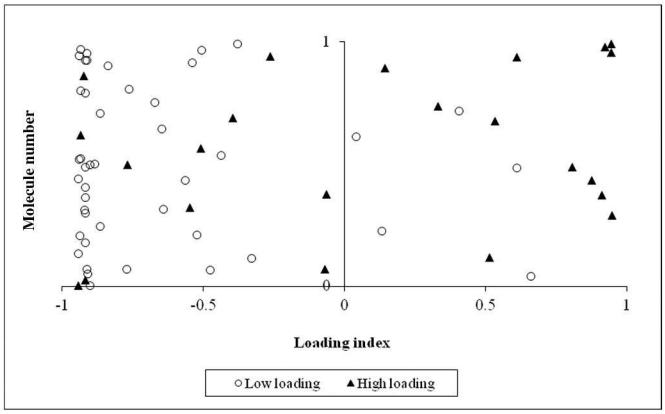

Fig. 1. External validation: index distribution, loading model (0.2/0.3 threshold structural descriptors).

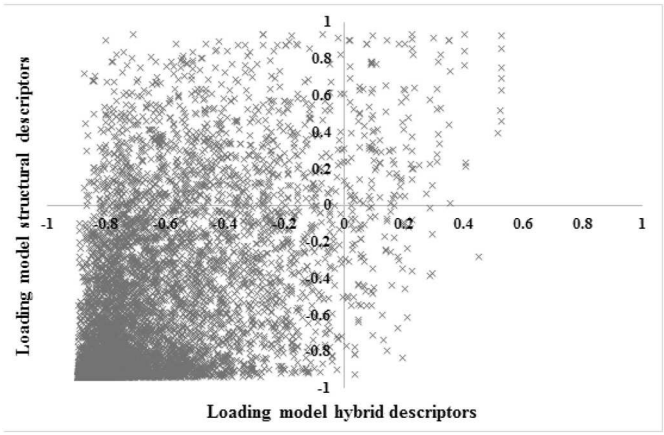

Fig. 2. Comparison between indexes of CMC screened molecules by the loading models: structural descriptors vs hybrid descriptors.

with increasing index values; at indexes ≥ 0.5, the false positive instances are 17% (2/12), and at indexes above 0.8, there are no false positive instances. Table 2 presents the descriptors that were found in >10% of the filters obtained for this model. The important descriptors were related to partial charges; PEOE_VSA-1 (54.4%) and PEOE_VSA_FHYD (29.8%). Other important descriptors were rotatable bonds (opr_nrot, b_rotN), sum of surface area of polar atoms (vsa_pol), topological polar surface area (TPSA), and others. The list of structural descriptors names and explanations may be found in Supplementary Table S3.

CMC and DB databases were screened by this model (based on 0.2/0.3 classification and structural descriptors). The screening results were compared to the screening obtained by the hybrid descriptors loading model (our previously published loading model [30]). Figs. 2 and 3 present the comparison. Table 3 summarizes these results. Screening by the new loading model resulted in ~14–15% of the molecules of both databases being identified as positives. This is a higher value than that obtained for the previous model (3–5%), probably due to broadening the classification of positives in the new model (see Section 2.1.2). The number of instances indexed above 0.5 (in the structural descriptors model), which is shown in the index distribution figure (Fig. 1) to have a lower false positive fraction, was much lower (248 and 293 for DB and CMC, respectively) which is 3.6% and 3.5% of the databases, respectively. Identifying molecules indexed above 0.5 will result in fewer chances of false positives, but at the expense of missing many true positive instances indexed between 0 and 0.5%. Most instances of positives in the hybrid model were also found to be positives in the screening by the structural model (61–64%), and 74–80% of the molecules that were indexed in the hybrid model ≥ 0.2 were also positives in the structural descriptors model. In Figs. 2 and 3, the lower right corner shows the few positive instances, that are positives by the hybrid descriptors loading model but negatives by the structural descriptors loading model. The good agreement between the screening results of the databases obtained by both models strengthens the predictability of the new model.

3.2. Leakage model

The leakage dataset, due to its smaller size, was modeled by ISE employing the "leave one out" (LOO) external validation scheme. In this scheme, the dataset was modeled with 26 molecules, and one

Table 2
Descriptors found in >10% of the filters in the loading model (0.2/0.3 threshold). A complete list of descriptors is found in Supplementary Table S3.

Descriptors	Descriptor category	Definition [32]	% Occurrence
PEOE_VSA-1[a]	Partial charge descriptors	The sum of van der Waals (VDW) surface area of atom i where the partial charge of atom i is in the range of −0.10 to −0.05	54.4
PEOE_VSA_FHYD[a]	Partial charge descriptors	Total hydrophobic VDW surface area	29.8
opr_nrot	Atom and bond counts	Rotatable bond count (Oprea method [89])	27.0
vsa_pol	Pharmacophore feature descriptors	Approximation to the sum of VDW surface areas of polar atoms	24.7
b_rotN	Atom and bond counts	Number of rotatable bonds	20.7
TPSA	Physical properties	Polar VDW surface area	19.4
a_ICM	Atom and bond counts	Atom information content (mean)	17.1
lip_don	Atom and bond counts	Lipinski donor count	17.0
BCUT_SMR_1[b]	Adjacency and distance matrix descriptors	The BCUT descriptors using atomic contribution to molar refractivity	16.3
a_nCl	Atom and bond counts	Number of chlorine atoms	14.1
BCUT_SMR_2[b]	Adjacency and distance matrix descriptors	The BCUT descriptors using atomic contribution to molar refractivity	12.8
PEOE_VSA_FPNEG[a]	Partial charge descriptors	Fractional negative VDW surface area	12.2
a_acc	Pharmacophore feature descriptor	Number of H-bond acceptor atoms	11.8
SMR_VSA1	Subdivided surface areas	The sum of VDW surface area of atom i where the molar refractivity is in the range of 0.11to 0.26	11.6
KierA1	Kier & Hall connectivity and kappa shape indices	First kappa shape index (connectivity index)	11.2
lip_acc	Atom and bond counts	Lipinski acceptor count	11.1
GCUT_SLOGP_0[b]	Adjacency and distance matrix descriptors	The GCUT descriptors using atomic contribution to logP	10.9
a_IC	Atom and bond counts	Atom information content (total)	10.4

[a] PEOE - The Partial Equalization of Orbital Electronegativities is a method of calculating atomic partial charges.
[b] BCUT and GCUT descriptors encode atomic properties relevant to intramolecular interactions.

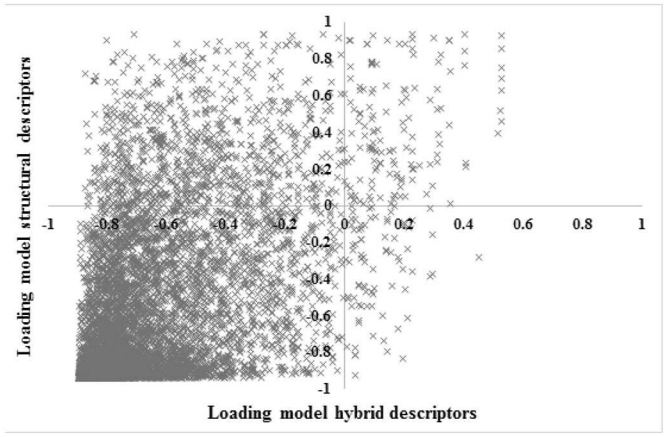

Fig. 3. Comparison between indexes of DB screened molecules by the loading models: structural descriptors vs hybrid descriptors.

molecule was tested as external. This process was repeated 27 times so that each molecule was tested once as an external. The external validation results are found in Table 4 and show high specificity (0.92) with only one false positive instance, and low sensitivity (0.47) with 8 false negative instances. Fig. 4 presents the distribution of the external validation index. As shown for the loading model, there is a trend in the index distribution of the externally validated molecules. The fraction of false negative instances was much lower at indexes below −0.5 (see the dotted line in Fig. 4). For positive instances, there was only one false positive molecule and its index value was 0.24. However, the misclassified positive instances (false negatives) were mainly indexed between −0.55 to zero. 71% of the instances in this range were false negatives. Changing the separating index from zero to −0.5 results in an increase in the sensitivity (0.73) at the expense of specificity (0.74). As explained for the loading model, in this case of a nano-liposomal delivery, testing the nano-liposomanl stability of a molecule is highly time and effort consuming, therefore we prefer to have the lowest possible number of false positives at the expense of high incidence of false negative instances. The separation index between positive and negative instances for the identification of candidates was therefore assigned at an index = 0.0.

Table 5 presents the descriptors found in >10% of the leakage filters. The most abundant filters were related to logP: GCUT_SLOGP_1 (40%) and GCUT_SLOGP_0 (38%), and to the partial charge negative surface area PEOE_VSA-3 (32%). Interestingly, the most important descriptors in the loading model (occurring in >20% of the filters) did not include logP-related descriptors, but were mainly related to partial charges. This is in agreement with the differences between loading and leakage processes. Loading is performed at a temperature above the Tm. The membrane at this temperature has a relatively large free volume, which allows for higher diffusion of the uncharged API, while the main driving force for loading is the ion gradient, which is affected mostly by the charge/polarity of the molecule. Therefore, loading will be somewhat less sensitive to the lipophilicity of the drug. Leakage from rigid membranes is a process occurring below the Tm of the phospholipids tested in this modeling approach (storage at 4 °C). Under these conditions, there is a small membrane free volume, and therefore the lipophilicity of a drug has a larger contribution to the process.

Table 3
Number of predicted positive instances and their percentage in CMC and DB databases by the hybrid vs structural descriptors loading models.

Model used/database screened	CMC		DB	
	No.	%	No.	%
Positive in structural descriptors loading model screening (current)	1159	14.4	1042	15.3
Molecules indexed above 0.5 in structural descriptors loading model screening (current)	293	3.5	248	3.6
Positive in hybrid loading model screening (previous)	425	5.1	221	3.2

Table 4
LOO cross-validation, leakage model.

	Zero index separating line		−0.5 index separating line	
	Obs rapid	Obs slow	Obs rapid	Obs slow
Pred rapid	11	8	9	4
Pred slow	1	7	3	11
% Correctly classified	66.67		74.10	
CCR	0.69		0.74	
Specificity	0.92		0.75	
Sensitivity	0.47		0.73	

To summarize, not surprisingly, the major descriptors in both loading and leakage processes are the degree of ionization combined with lipophilicity, which are very similar in both directions (loading and leakage). What differs between the two processes is only the membrane "free volume", which is high at a temperature above the Tm (loading) and low at a temperature below the Tm (leakage). This difference was reflected in the important descriptors found for both modeled characteristics.

The leakage model was used to screen CMC and DB databases. In addition, the DB database contains 1714 molecules that are already FDA-approved, and those molecules were also screened separately. The screening results are summarized in Table 6. These results were compared to the indexes resulting from screening using the loading model (structural descriptors). The comparisons are found in Figs. 5 and 6. The results show that the fraction of positives across the databases is similar, with 14.4–16.6% positives by the loading model and 7.2–10.4% positives by the leakage model. 4.7–6.3% of the databases are predicted to be positives by both models. Among this group, 91 molecules are duplicates, which results in 667 unique molecules predicted to be positives by both models. High-scored molecules are defined as those having an index above zero in the leakage model and above 0.5 in the loading model. The loading model shows a lower false positive fraction at indexes ≥ 0.5 in the external validation (Fig. 1). This group of molecules accounts for 2.4% (318 unique drugs, after removing duplicates) of the databases and 3.9% of the FDA-approved drugs in DB (67 drugs). Fig. 7 shows the high-scored molecules in the approved DB. The red dots in the figure represent drugs that are found in the datasets used for model building (8 drugs). Other drugs in this figure come from different pharmacological groups (antibiotics, antivirals, anticancers, and other). This group of drugs may be the basis for new liposomal drugs.

Table 6 presents also the estimated number of false positives and false negative instances in each database screening. As explained earlier,

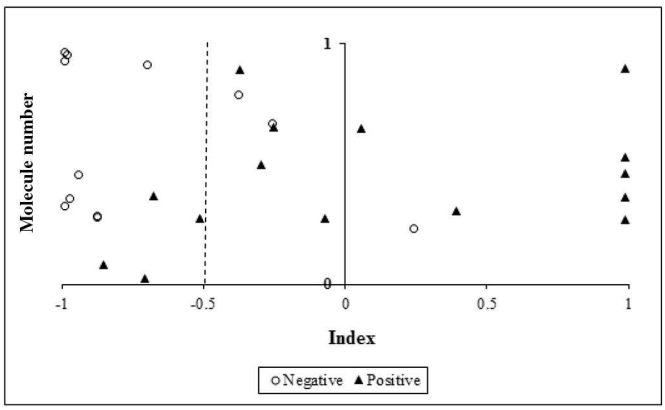

Fig. 4. External test indexes distribution, leakage model.

Table 5
Descriptors found in >10% of the filters in leakage model. A complete list of descriptors is found in Supplementary Table S3.

Descriptors	Descriptor category	Definition [32]	% Occurrence
GCUT_SLOGP_1	Adjacency and distance matrix descriptors	The GCUT descriptors using atomic contribution to logP	40.0
GCUT_SLOGP_0	Adjacency and distance matrix descriptors	The GCUT descriptors using atomic contribution to logP	38.0
PEOE_VSA-3	Partial charge descriptors	The sum of van der Waals (VDW) surface area of atom i where the partial charge of atom i is in the range of −0.20 to-0.15	31.5
SMR_VSA1	Subdivided surface areas	The sum of VDW surface area of atom i where the molar refractivity is in the range of 0.11–0.26	28.2
GCUT_PEOE_3	Adjacency and distance matrix descriptors	The GCUT descriptors using atomic contribution to the PEOE partial charges	25.6
bpol	Physical properties	Difference of bonded atom polarizabilities	25.5
a_acc	Pharmacophore feature descriptor	Number of H-bond acceptor atoms	25.1
BCUT_SLOGP_2	Adjacency and distance matrix descriptors	The BCUT descriptors using atomic contribution to logP	24.8
a_nP	Atom and bond counts	Number of phosphorus atoms	23.1
a_nCl	Atom and bond counts	Number of chlorine atoms	16.7
KierA2	Kier & Hall connectivity and kappa shape indices	First kappa shape index (connectivity index)	16.4
PEOE_VSA-0	Partial charge descriptors	The sum of VDW surface area of atom i where the partial charge of atom i is in the range of −0.05 to 0	16.2
a_nF	Atom and bond counts	Number of fluorine atoms	16.0
GCUT_SLOGP_2	Adjacency and distance matrix descriptors	The GCUT descriptors using atomic contribution to logP	16.0
a_nH	Atom and bond counts	Number of hydrogen atoms	14.8
PEOE_VSA_POS	Partial charge descriptors	Total positive VDW surface area	14.5
TPSA	Physical properties	Polar VDW surface area	14.0
PEOE_VSA-2	Partial charge descriptors	The sum of van der Waals (VDW) surface area of atom i where the partial charge of atom i is in the range of-0.15 to-0.10	13.2
b_count	Atom and bond counts	Number of bonds	12.7

a- PEOE - The Partial Equalization of Orbital Electronegativities is a method of calculating atomic partial charges.
b- BCUT and GCUT descriptors encode atomic properties relevant to intramolecular interactions.

the fraction of false negative instances expected by the use of leakage model screening is high, however the estimated number of false positives is low which is highly important in our screening due to the associated lengthy experimental validations. The number of false positive instances is higher for the loading model and this number may be decreased by identifying the high scored candidates with loading score ≥ 0.5.

4. Conclusions

Modeling suitability of drugs for delivery by nano-liposomes has already proven its advantages for liposomal drug design [23–25]. In this study we improved the model by focusing on liposomal formulations based on liposomes with lipid bilayers which are at the liquid ordered (LO) phase that are based on high-T_m (above 37 °C) "liposome forming" PCs such as HSPC, and on high mole% cholesterol (≥30 mole%). The high cholesterol content is responsible for transforming the lipid bilayer to a LO phase [33] and is critical to achieve the desired liposome stability upon storage and during in vivo blood circulation. This liposome composition is the most common for liposomal formulations currently used and most of the available data are related to this range of lipid composition. In addition, as this composition is the most applied currently, screening molecules suitability for this type of formulation would be most advantageous. Having enough data on other liposomal compositions will allow to develop models for different liposomal compositions. The new models were thus constructed based only on the structural properties of the APIs and the resulting models are capable of predicting both remote loading and leakage of drugs, which are both required for any useful future liposomal formulation.

As the liposome lipid composition and size distribution were kept similar, experimentally derived descriptors (EDD) were not used for model building. This allows the models to focus on the properties of the API itself, giving these properties greater weight in the models. Interestingly, it was found that the most prevalent descriptors in the loading models were mainly related to the partial charge and polar region of the API, while the most important descriptors in the leakage models were those related to logP. These findings are in agreement with the differences between loading and leakage processes. Loading is performed at a temperature above the T_m. The membrane at this temperature has a relatively large free volume, which allows for higher diffusion of the

Table 6
Number of predicted positive instances in CMC and DB databases by the loading and leakage models based on structural descriptors.

	CMC (8402 molecules)				DB (6831 molecules)				Approved DB (1714 molecules)			
	No. of positives	% Positives	Estimated no. of FP	Estimated no. of FN	No. of positives	% positives	Estimated no. of FP	Estimated no. of FN	No. of positives	% positives	Estimated no. of FP	Estimated no. of FN
Loading model	1159	14.4	341	1593	1042	15.3	306	1274	284	16.6	83	315
Loading model, high scored (positive instances indexed ≥ 0.5)	293	3.5	49	1914	248	3.6	41	1554	63	3.7	10	390
Leakage model	768	9.1	96	3054	493	7.2	62	2535	178	10.4	22	614
Positive in both loading and leakage models	439	5.2			319	4.7			108	6.3		
High scored instances. Indexed ≥ 0.5 in loading and above zero in leakage models	205	2.4			161	2.4			67	3.9		

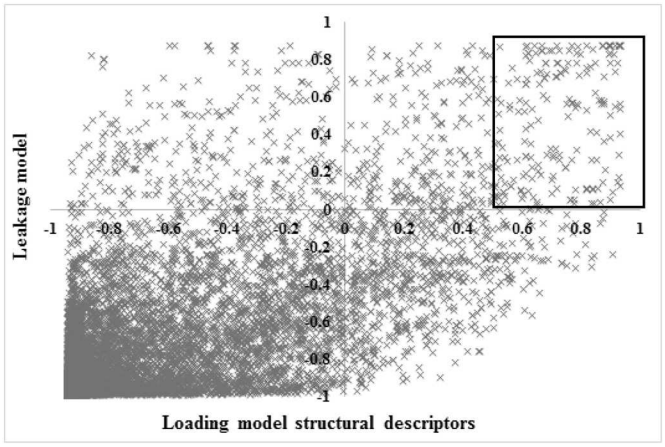

Fig. 5. Comparison between screening molecules index in CMC database in the loading and leakage models. Rectangle in upper right corner represents high-score instances.

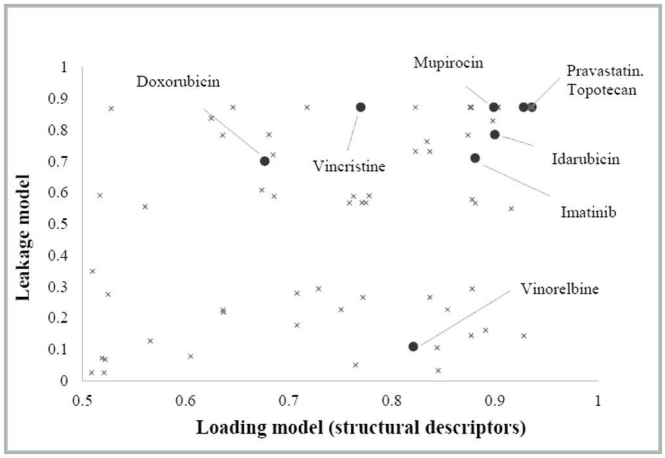

Fig. 7. Comparison between screening molecules index in the loading and leakage models of high-scored drugs, which are FDA-approved drugs in DB database. The dots are molecules found in the datasets used for model building.

uncharged amphipathic API, and the main driving force for loading is the ion gradient, whose effectiveness is based on the charge/polarity of the molecule. Therefore loading will be less sensitive to the lipophilicity of the drug. Leakage from liposomes based on high T_m PC upon storage at 4 °C occurs much below the T_m of the phospholipids (≥37 °C). Under such conditions, there is only a small membrane "free volume", and therefore the lipophilicity of the drugs has a larger contribution to the process. Screening two large molecular databases by the new models resulted in 667 molecules predicted to be positives for their loading and leakage properties. 318 molecules in this group were defined as high-scored molecules, and 67 of those molecules are FDA-approved drugs. It should be noted that our models are focused on obtaining high specificity of the model i.e. having the lowest number of false negative instances, which in our case was at the expense of a high fraction of false negative instances. Screening by the loading model therefore results in 22% false negative instances out of all negatives (low loading) instances and the leakage model results in 40% false negatives out of the predicted negative group. However, the false positive instances are lower with 17% false positives in the high scored loading positives and 12.5% in the slow predicted instances. As discussed in our previous publication [23], the computational screening is the first screening, which requires further considerations related to liposomal drug design for the selection of a drug for nano-liposomal delivery. These considerations consist of the following: (1) The disease for which the drug is intended should benefit from the EPR effect; (2) Evaluation of the advantages that the liposomal delivery system has for the specific molecule; (3) Dose per single administration should not exceed 200 mg. An additional prerequisite is that the selected drug meets the requirements of being an amphipathic weak acid or base. Investigating the group of 67 molecules from the approved DB database that were highly scored by the models, molecules with diverse approved indications were found: for treatments of migraine, asthma, cancer, bacterial infections, HIV, pain and more. A deeper literature search revealed additional indications for some of these molecules that are not labeled indications; in many cases, these additional indications may gain value from formulating the drug in nano-liposomes. This paper shows the advantages of using a computational approach to identify molecules suitable for liposomal delivery. These comprised 2.4–3.9% of the screened drugs. This coarse screening should be followed by a thorough specific evaluation of the candidates obtained. The model presented may also be used to test the suitability of a specific molecule and for the design of certain modifications to the drug that will make it suitable for this drug delivery system. This approach improves the process of developing and the chances for successful nano-drug formulations.

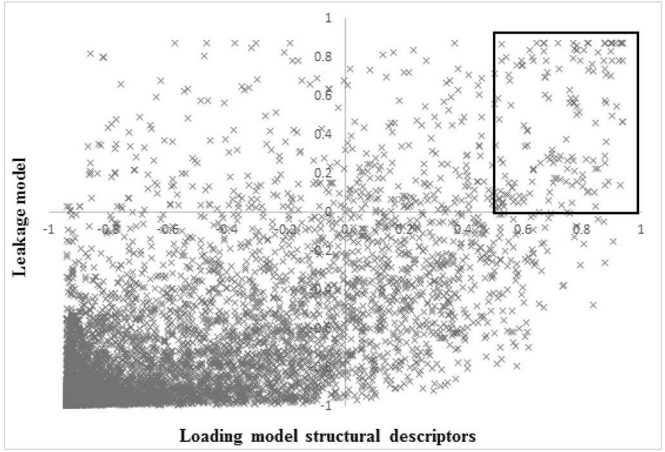

Fig. 6. Comparison between screening molecules index in DB database in the loading and leakage models. Black rectangle represents high-score instances.

Acknowledgments

This study was supported by the Barenholz Fund at the Hebrew University of Jerusalem. This fund originated from royalties Hebrew University received from Yechezkel Barenholz's commercialized projects. Part of this money is used to support the research activities of Barenholz Lab. We authors would like to thank Mr. Sigmund Geller for editing this paper.

Appendix A. Supplementary data

Supplementary data to this article can be found online at http://dx.doi.org/10.1016/j.jconrel.2017.02.015.

References

[1] Y. Barenholz, Doxil®—the first FDA-approved nano-drug: lessons learned, J. Control. Release 160 (2012) 117–134.
[2] Y. Barenholtz, Doxil®: the first FDA-approved nano-drug, Handb. Clin. Nanomedicine, Pan Stanford Publishing Pte Ltd, 2015.
[3] T.M. Allen, P.R. Cullis, Liposomal drug delivery systems: from concept to clinical applications, Adv. Drug Deliv. Rev. 65 (2013) 36–48, http://dx.doi.org/10.1016/j.addr.2012.09.037.
[4] H.-I. Chang, M.-K. Yeh, Clinical development of liposome-based drugs: formulation, characterization, and therapeutic efficacy, Int. J. Nanomedicine 7 (2012) 49–60, http://dx.doi.org/10.2147/IJN.S26766.

[5] V. Wagner, A. Dullaart, A.K. Bock, A. Zweck, The emerging nanomedicine landscape, Nat. Biotechnol. 24 (2006) 1211–1217, http://dx.doi.org/10.1038/nbt1006/1211.

[6] A.J. Huh, Y.J. Kwon, "Nanoantibiotics": a new paradigm for treating infectious diseases using nanomaterials in the antibiotics resistant era, J. Control. Release 156 (2011) 128–145, http://dx.doi.org/10.1016/j.jconrel.2011.07.002.

[7] AmBisome (amphotericin B) liposome for injection, 2012.

. [8] R. Parboosing, G.E.M. Maguire, P. Govender, H.G. Kruger, Nanotechnology and the treatment of HIV infection, Viruses 4 (2012) 488–520, http://dx.doi.org/10.3390/v4040488.

[9] T. Mamo, E.A. Moseman, N. Kolishetti, C. Salvador, J. Shi, D.R. Kuritzkes, et al., Emerging nanotechnology approaches for HIV/AIDS treatment and prevention, 5 (2010) 269–285. doi: 10.2217/nnm.10.1.Emerging.

.[10] K. Turjeman, Y. Bavli, P. Kizelsztein, Y. Schilt, N. Allon, T.B. Katzir, et al., Nano-drugs based on nano sterically stabilized liposomes for the treatment of inflammatory neurodegenerative diseases, PLoS One 10 (2015), e0130442. http://dx.doi.org/10.1371/journal.pone.0130442.

[11] H. Maeda, G.Y. Bharate, J. Daruwalla, Polymeric drugs for efficient tumor-targeted drug delivery based on EPR-effect, Eur. J. Pharm. Biopharm. 71 (2009) 409–419, http://dx.doi.org/10.1016/j.ejpb.2008.11.010.

[12] E.A. Azzopardi, E.L. Ferguson, D.W. Thomas, The enhanced permeability retention effect: a new paradigm for drug targeting in infection, J. Antimicrob. Chemother. 68 (2013) 257–274, http://dx.doi.org/10.1093/jac/dks379.

[13] H. Maeda, J. Fang, T. Inutsuka, Y. Kitamoto, Vascular permeability enhancement in solid tumor: various factors, mechanisms involved and its implications, Int. Immunopharmacol. 3 (2003) 319–328, http://dx.doi.org/10.1016/S1567-5769(02)00271-0.

[14] H. Maeda, J. Wu, T. Sawa, Y. Matsumura, K. Hori, Tumor vascular permeability and the EPR effect in macromolecular therapeutics: a review, J. Control. Release 65 (2000) 271–284, http://dx.doi.org/10.1016/S0168-3659(99)00248-5.

[15] Y. Barenholz, Relevancy of drug loading to liposomal formulation therapeutic efficacy, J. Lipid Res. 13 (2003) 1–8.

[16] G. Haran, R. Cohen, L.K. Bar, Y. Barenholz, Transmembrane ammonium sulfate gradients in liposomes produce efficient and stable entrapment of amphipathic weak bases, Biochim. Biophys. Acta 1151 (1993) 201–215http://www.ncbi.nlm.nih.gov/pubmed/8373796.

[17] S. Clerc, Y. Barenholz, Loading of amphipathic weak acids into liposomes in response to transmembrane calcium acetate gradients, Biochim. Biophys. Acta 1240 (1995) 257–265.

[18] D. Zucker, D. Marcus, Y. Barenholz, A. Goldblum, Liposome drug's loading efficiency: a working model based on loading conditions and drug's physicochemical properties, J. Control. Release 139 (2009) 73–80.

[19] D. Zucker, A.V. Andriyanov, A. Steiner, U. Raviv, Y. Barenholz, Characterization of PEGylated nanoliposomes co-remotely loaded with topotecan and vincristine: relating structure and pharmacokinetics to therapeutic efficacy, J. Control. Release 160 (2012) 281–289, http://dx.doi.org/10.1016/j.jconrel.2011.10.003.

[20] Y. Avnir, K. Turjeman, D. Tulchinsky, A. Sigal, P. Kizelsztein, D. Tzemach, et al., Fabrication principles and their contribution to the superior in vivo therapeutic efficacy of nano-liposomes remote loaded with glucocorticoids, PLoS One 6 (2011), e25721. http://dx.doi.org/10.1371/journal.pone.0025721.

[21] V. Wasserman, P. Kizelsztein, O. Garbuzenko, R. Kohen, H. Ovadia, R. Tabakman, et al., The antioxidant tempamine: in vitro antitumor and neuroprotective effects and optimization of liposomal encapsulation and release, Langmuir 23 (2007) 1937–1947, http://dx.doi.org/10.1021/la060218k.

[22] Y. Avnir, R. Ulmansky, V. Wasserman, S. Even-Chen, M. Broyer, Y. Barenholz, et al., Amphipathic weak acid glucocorticoid prodrugs remote-loaded into sterically stabilized nanoliposomes evaluated in arthritic rats and in a Beagle dog: a novel approach to treating autoimmune arthritis, Arthritis Rheum. 58 (2008) 119–129.

[23] A. Cern, Y. Barenholz, A. Tropsha, A. Goldblum, Computer-aided design of liposomal drugs: in silico prediction and experimental validation of drug candidates for liposomal remote loading, J. Control. Release 173 (2014) 125–131.

[24] A. Cern, E. Nativ-Roth, A. Goldblum, Y. Barenholz, Effect of solubilizing agents on mupirocin loading into and release from PEGylated nanoliposomes, J. Pharm. Sci. (2014) 1–8, http://dx.doi.org/10.1002/jps.24037.

[25] A. Cern, A. Michael-Gayego, Y. Bavli, E. Koren, A. Goldblum, A.E. Moses, et al., Nano-mupirocin: enabling the parenteral activity of mupirocin, Eur. J. Nanomed. 8 (2016) 139–149.

[26] L. Silverman, Y. Barenholz, In vitro experiments showing enhanced release of doxorubicin from Doxil® in the presence of ammonia may explain drug release at tumor site, Nanomedicine 11 (2015) 1841–1850, http://dx.doi.org/10.1016/j.nano.2015.06.007.

[27] Y. Avnir, K. Turjeman, D. Tulchinsky, A. Sigal, P. Kizelsztein, D. Tzemach, et al., Fabrication principles and their contribution to the superior in vivo therapeutic efficacy of nano-liposomes remote loaded with glucocorticoids, PLoS One 6 (2011), e25721. http://dx.doi.org/10.1371/journal.pone.0025721.

[28] J.H. Waknine-Grinberg, S. Even-Chen, J. Avichzer, K. Turjeman, A. Bentura-Marciano, R.K. Haynes, et al., Glucocorticosteroids in nano-sterically stabilized liposomes are efficacious for elimination of the acute symptoms of experimental cerebral malaria, PLoS One 8 (2013), e72722. http://dx.doi.org/10.1371/journal.pone.0072722.

[29] S. Sur, A.C. Fries, K.W. Kinzler, S. Zhou, B. Vogelstein, Remote loading of preencapsulated drugs into stealth liposomes, Proc. Natl. Acad. Sci. U. S. A. 111 (2014) 2283–2288, http://dx.doi.org/10.1073/pnas.1324135111.

[30] A. Cern, A. Golbraikh, A. Sedykh, A. Tropsha, Y. Barenholz, A. Goldblum, Quantitative structure - property relationship modeling of remote liposome loading of drugs, J. Control. Release 160 (2012) 147–157.

[31] D.C. Drummond, C.O. Noble, M.E. Hayes, J.W. Park, D.B. Kirpotin, Pharmacokinetics and in vivo drug release rates in liposomal nanocarrier development, J. Pharm. Sci. (2008)http://dx.doi.org/10.1002/jps.

[32] MOE, 2012.10, Molecular Operating Environment, http://www.chemcomp.com/index.htm 2012.

[33] O.G. Mouritsen, Life as a Matter of Fat: The Emerging Science of Lipidomics, Springer, Berlin, 2005.

[34] K. Shimizu, M. Takada, T. Asai, K. Kuromi, K. Baba, N. Oku, Cancer chemotherapy by liposomal 6-[12-(dimethylamino)ethyl]aminol-3-hydroxy-7H-indeno[2,1-clquinolin-7-one dihydrochloride] (TAS-103), a novel anti-cancer agent, Biol. Pharm. Bull. 25 (2002) 1385–1387http://www.ncbi.nlm.nih.gov/pubmed/12392102.

[35] G. Stensrud, S.A. Sande, S. Kristensen, G. Smistad, Formulation and characterisation of primaquine loaded liposomes prepared by a pH gradient using experimental design, Int. J. Pharm. 198 (2000) 213–228http://www.ncbi.nlm.nih.gov/pubmed/10767570.

[36] C. Chemin, J.M. Pean, C. Bourgaux, G. Pabst, P. Wuthrich, P. Couvreur, et al., Supramolecular organization of S12363-liposomes prepared with two different remote loading processes, Biochim. Biophys. Acta 1788 (2009) 926–935, http://dx.doi.org/10.1016/j.bbamem.2008.11.017.

[37] Y. Maitani, SungHee Hwang, Xian-Rong Qi, Kozo Takayama, Tsuneji Nagai, Remote loading of diclofenac, insulin and fluorescein isothiocyanate labeled insulin into liposomes by pH and acetate gradient methods, Int. J. Pharm. 179 (1999) 85–95.

[38] G. Urbinati, D. Audisio, V. Marsaud, V. Plassat, S. Arpicco, B. Sola, et al., Therapeutic potential of new 4-hydroxy-tamoxifen-loaded pH-gradient liposomes in a multiple myeloma experimental model, Pharm. Res. 27 (2010) 327–339, http://dx.doi.org/10.1007/s11095-009-0023-z.

[39] L. Krugner-Higby, B. KuKanich, B. Schmidt, T.D. Heath, C. Brown, L.J. Smith, Pharmacokinetics and behavioral effects of an extended-release, liposome-encapsulated preparation of oxymorphone in rhesus macaques, J. Pharmacol. Exp. Ther. 330 (2009) 135–141, http://dx.doi.org/10.1124/jpet.108.150052.

[40] S. Tu, T. McGinnis, L. Krugner-Higby, T.D. Heath, A mathematical relationship for hydromorphone loading into liposomes with trans-membrane ammonium sulfate gradients, J. Pharm. Sci. 99 (2010) 2672–2680, http://dx.doi.org/10.1002/jps.22017.

[41] M. Celano, M.G. Calvagno, S. Bulotta, D. Paolino, F. Arturi, D. Rotiroti, et al., Cytotoxic effects of gemcitabine-loaded liposomes in human anaplastic thyroid carcinoma cells, BMC Cancer 4 (2004) 63, http://dx.doi.org/10.1186/1471-2407-4-63.

[42] F. FrÉZard, A. Garnier-Suillerot, C. Demicheli, Encapsulation of mithramycin in liposomes in response to a transmembrane gradient of calcium ions, J. Incl. Phenom. Macrocycl. Chem. 28 (1997) 51–62, http://dx.doi.org/10.1023/a:1007985811673.

[43] N. Dos Santos, L.D. Mayer, S.A. Abraham, R.C. Gallagher, K.A. Cox, P.G. Tardi, et al., Improved retention of idarubicin after intravenous injection obtained for cholesterol-free liposomes, Biochim. Biophys. Acta 1561 (2002) 188–201http://www.ncbi.nlm.nih.gov/pubmed/11997119.

[44] T.D. Madden, P.R. Harrigan, L.C. Tai, M.B. Bally, L.D. Mayer, T.E. Redelmeier, et al., The accumulation of drugs within large unilamellar vesicles exhibiting a proton gradient: a survey, Chem. Phys. Lipids 53 (1990) 37–46http://www.ncbi.nlm.nih.gov/pubmed/1972352.

[45] I.V. Zhigaltsev, G. Winters, M. Srinivasulu, J. Crawford, M. Wong, L. Amankwa, et al., Development of a weak-base docetaxel derivative that can be loaded into lipid nanoparticles, J. Control. Release 144 (2010) 332–340, http://dx.doi.org/10.1016/j.jconrel.2010.02.029.

[46] L. Jia, M. Garza, H. Wong, D. Reimer, T. Redelmeier, J.B. Camden, et al., Pharmacokinetic comparison of intravenous carbendazim and remote loaded carbendazim liposomes in nude mice, J. Pharm. Biomed. Anal. 28 (2002) 65–72http://www.ncbi.nlm.nih.gov/pubmed/11861109.

[47] T. Wiens, T. Redelmeier, Y. Av-Gay, Development of a liposome formulation of ethambutol, Antimicrob. Agents Chemother. 48 (2004) 1887–1888, http://dx.doi.org/10.1128/aac.48.5.1887-1888.2004.

[48] L. Qiu, N. Jing, Y. Jin, Preparation and in vitro evaluation of liposomal chloroquine diphosphate loaded by a transmembrane pH-gradient method, Int. J. Pharm. 361 (2008) 56–63, http://dx.doi.org/10.1016/j.ijpharm.2008.05.010.

[49] K. Shimizu, M. Takada, T. Asai, K. Irimura, K. Baba, N. Oku, Potential usage of liposomal 4beta-aminoalkyl-4′-O-demethyl-4-desoxypodophyllotoxin (TOP-53) for cancer chemotherapy, Biol. Pharm. Bull. 25 (2002) 783–786http://www.ncbi.nlm.nih.gov/pubmed/12081147.

[50] U. Glaberman, I. Rabinowitz, C.F. Verschraegen, Alternative administration of camptothecin analogues, Expert Opin. Drug Deliv. 2 (2005) 323–333, http://dx.doi.org/10.1517/17425247.2.2.323.

[51] J.L. Slater, G.T. Colbern, P.K. Working, Liposome-entrapped topoisomerase inhibitors, USA Pat. (2007).

.[52] Liposome composition and method for administrating a quinolone, PCT. (1999).

.[53] A.K. Rajput, P. Jain, Development and characterization of citicholine, Int. J. Pharm. Prof. Res. 1 (2010) 81–84.

[54] M.A. Rajnarayan, G.N. Ishwarlal, B.M. Ramgopal, S.B. Babulal, S.R. Shantaram, J.A.S. Pinjari, Liposomal Citicoline Injection, PCT. (2010).

.[55] M.E. Hayes, C.O. Noble, F.C.J. Szoka, Remote loading of sparingly water-soluble drugs into liposomes, 2014.

.[56] S. Du, Y. Deng, Studies on the encapsulation of oxymatrine into liposomes by ethanol injection and pH gradient method, Drug Dev. Ind. Pharm. 32 (2006) 791–797, http://dx.doi.org/10.1080/03639040600760556.

[57] J. Chen, A. Lin, Z. Chen, W. Wang, T. Zhang, H. Cai, et al., Ammonium sulfate gradient loading of brucine into liposomes: effect of phospholipid composition on entrapment efficiency and physicochemical properties in vitro, Drug Dev. Ind. Pharm. 36 (2010) 245–253, http://dx.doi.org/10.1080/03639040903099736.

[58] M.M. Gaspar, A. Cruz, A.F. Penha, J. Reymão, A.C. Sousa, C.V. Eleutério, et al., Rifabutin encapsulated in liposomes exhibits increased therapeutic activity in a model of disseminated tuberculosis, Int. J. Antimicrob. Ag. 31 (2008) 37–45, http://dx.doi.org/10.1016/j.ijantimicag.2007.08.008.
[59] A. Wagner, K. Vorauer-Uhl, H. Katinger, Liposomal composition comprising an active ingredient for relaxing smooth muscle, the production of this composition and the therapeutic use thereof, USA Pat. (2009).
.[60] A.C. Pinto, J.N. Moreira, S. Simoes, Liposomal imatinib-mitoxantrone combination: formulation development and therapeutic evaluation in an animal model of prostate cancer, Prostate 71 (2011) 81–90, http://dx.doi.org/10.1002/pros.21224.
[61] B.J. Tan, K.S. Quek, M.Y. Wong, W.K. Chui, G.N. Chiu, Liposomal M-V-05: formulation development and activity testing of a novel dihydrofolate reductase inhibitor for breast cancer therapy, Int. J. Oncol. 37 (2010) 211–218http://www.ncbi.nlm.nih.gov/pubmed/20514413.
[62] J. Wang, B. Goh, W. Lu, Q. Zhang, A. Chang, X.Y. Liu, et al., In vitro cytotoxicity of stealth liposomes co-encapsulating doxorubicin and verapamil on doxorubicin-resistant tumor cells, Biol. Pharm. Bull. 28 (2005) 822–828http://www.ncbi.nlm.nih.gov/pubmed/15863886.
[63] C.L. Li, J.X. Cui, C.X. Wang, L. Zhang, Y.H. Li, X. Xiu, et al., Development of pegylated liposomal vinorelbine formulation using "post-insertion" technology, Int. J. Pharm. 391 (2010) 230–236, http://dx.doi.org/10.1016/j.ijpharm.2010.03.004.
[64] J. Qin, D. Chen, W. Lu, H. Xu, C. Yan, H. Hu, et al., Preparation, characterization, and evaluation of liposomal ferulic acid in vitro and in vivo, Drug Dev. Ind. Pharm. 34 (2008) 602–608, http://dx.doi.org/10.1080/03639040701833559.
[65] J.C.-L. Ong, F. Sun, E. Chan, Development of stealth liposome coencapsulating doxorubicin and fluoxetine, J. Lipid Res. 21 (2011) 261–271, http://dx.doi.org/10.3109/08982104.2010.545070.
[66] K. Hironaka, Y. Inokuchi, T. Fujisawa, H. Shimazaki, M. Akane, Y. Tozuka, et al., Edaravone-loaded liposomes for retinal protection against oxidative stress-induced retinal damage, Eur. J. Pharm. Biopharm. 79 (2011) 119–125, http://dx.doi.org/10.1016/j.ejpb.2011.01.019.
[67] R. Lee, X. Zhou, B. Yung, Y. Huang, H. Li, X. Hu, G. Xiang, Novel liposomal gefitinib (L-GEF) formulations, Anticancer Res. 32 (7) (2012) 2919–2923.
[68] P. Luciani, M. Fevre, J.-C. Leroux, Development and physico-chemical characterization of a liposomal formulation of istaroxime, Eur. J. Pharm. Biopharm. 79 (2011) 285–293, http://dx.doi.org/10.1016/j.ejpb.2011.04.013.
[69] K. Hironaka, T. Fujisawa, H. Sasaki, Y. Tozuka, K. Tsuruma, M. Shimazawa, et al., Fluorescence investigation of the retinal delivery of hydrophilic compounds via liposomal eyedrops, Biol. Pharm. Bull. 34 (2011) 894–897http://www.ncbi.nlm.nih.gov/pubmed/21628890.
[70] K. Muppidi, A.S. Pumerantz, J. Wang, G. Betageri, Development and stability studies of novel liposomal vancomycin formulations, ISRN Pharm. 2012 (2012) 636743, http://dx.doi.org/10.5402/2012/636743.
[71] S. Modi, T.-X. Xiang, B.D. Anderson, Enhanced active liposomal loading of a poorly soluble ionizable drug using supersaturated drug solutions, J. Control. Release 162 (2012) 330–339, http://dx.doi.org/10.1016/j.jconrel.2012.07.001.
[72] Y. Liu, S.D. Yoo, L. Li, L. Fang, Z. Wen, T. Li, Formulation and characterization of boanmycin-loaded liposomes prepared by pH gradient experimental design, Drug Deliv. 19 (2012) 90–101, http://dx.doi.org/10.3109/10717544.2011.649217.
[73] F. Sun, J. Li, Q. Yu, E. Chan, Loading 3-deazaneplanocin A into pegylated unilamellar liposomes by forming transient phenylboronic acid-drug complex and its pharmacokinetic features in Sprague-Dawley rats, Eur. J. Pharm. Biopharm. 80 (2012) 323–331, http://dx.doi.org/10.1016/j.ejpb.2011.10.014.
[74] C. Giuliani, B. Altieri, C. Bombelli, L. Galantini, G. Mancini, A. Stringaro, Remote loading of aloe emodin in gemini-based cationic liposomes, Langmuir 31 (2015) 76–82, http://dx.doi.org/10.1021/la5038074.
[75] E. See, W. Zhang, J. Liu, D. Svirskis, B.C. Baguley, J.P. Shaw, et al., Physicochemical characterization of asulacrine towards the development of an anticancer liposomal formulation via active drug loading: stability, solubility, lipophilicity and ionization, Int. J. Pharm. 473 (2014) 528–535, http://dx.doi.org/10.1016/j.ijpharm.2014.07.033.
[76] T. Ishida, Y. Takanashi, H. Doi, I. Yamamoto, H. Kiwada, Encapsulation of an antivasospastic drug, fasudil, into liposomes, and in vitro stability of the fasudil-loaded liposomes, Int. J. Pharm. 232 (2002) 59–67http://www.ncbi.nlm.nih.gov/pubmed/11790490.
[77] X. Zhang, P. Sun, R. Bi, J. Wang, N. Zhang, G. Huang, Targeted delivery of levofloxacin-liposomes for the treatment of pulmonary inflammation, J. Drug Target. 17 (2009) 399–407, http://dx.doi.org/10.1080/10611860902795407.
[78] C. Engelmann, Y. Panis, J. Bolard, B. Diquet, M. Fabre, H. Nagy, et al., Liposomal encapsulation of ganciclovir enhances the efficacy of herpes simplex virus type 1 thymidine kinase suicide gene therapy against hepatic tumors in rats, Hum. Gene Ther. 10 (1999) 1545–1551, http://dx.doi.org/10.1089/10430349950017879.
[79] F. Frezard, N.M. Silva-Barcellos, A.L. de Melo, Schistosomicidal Activity of Oxamniquine Encapsulated in Sterically Stabilized Liposomes: Influence of the Route of Administration, XVI Congr. Bras, Parasitol, 1999.
[80] I.V. Zhigaltsev, A.P. Kaplun, V.G. Kucheryanu, G.N. Kryzhanovsky, S.N. Kolomeichuk, V.I. Shvets, et al., Liposomes containing dopamine entrapped in response to transmembrane ammonium sulfate gradient as carrier system for dopamine delivery into the brain of parkinsonian mice, J. Liposome Res. 11 (2001) 55–71, http://dx.doi.org/10.1081/LPR-100103170.
[81] Guidance for Industry Drug Stability Guidelines, 2008.
[82] S.C. Semple, A. Chonn, P.R. Cullis, Interactions of liposomes and lipid-based carrier systems with blood proteins: relation to clearance behaviour in vivo, Adv. Drug Deliv. Rev. 32 (1998) 3–17, http://dx.doi.org/10.1016/S0169-409X(97)00128-2.
[83] D. Liu, F. Zhou, L. Huang, Characterization of plasma-stabilized liposomes composed of dioleoyl-phosphatidylethanolamine and oleic acid, Biochem. Biophys. Res. Commun. 162 (1989) 326–333.
[84] D. Cosco, M.G. Calvagno, Christian Celia, Donatella Paolino, P. Doldo, M. Frest, Michelangelo Iannone, Francesco Castelli, Effects of lipid composition and preparation conditions on physical- chemical properties, technological parameters and in vitro biological activity of gemcitabine-loaded liposomes, Curr. Drug Deliv. 4 (2007) 89–101.
[85] M. Chen, J. Chen, T. Hou, Y. Fang, W. Sun, R. Hu, et al., Effect of phospholipid composition on pharmaceutical properties and anti-tumor activity of stealth liposomes containing brucine, Zhongguo Zhong Yao Za Zhi 36 (2011) 864–867http://www.ncbi.nlm.nih.gov/pubmed/21761723.
[86] C. Li, J. Cui, C. Wang, Y. Li, H. Zhang, J. Wang, et al., Encapsulation of mitoxantrone into pegylated SUVs enhances its antineoplastic efficacy, Eur. J. Pharm. Biopharm. 70 (2008) 657–665, http://dx.doi.org/10.1016/j.ejpb.2008.05.019.
[87] Doxil Product Information, http://www.doxil.com/ 2013.
[88] N. Stern, A. Goldblum, Iterative Stochastic Elimination for solving complex combinatorial problems in drug discovery, Israel J. Chem. 54 (2014) 1338–1357, http://dx.doi.org/10.1002/ijch.201400072.
[89] T.I. Oprea, Property distribution of drug-related chemical databases, J. Comput. Aided Mol. Des. 14 (2000) 251–264, http://dx.doi.org/10.1023/A:1008130001697.